A compact rotating-mirror autocorrelator design for femtosecond and picosecond laser pulses

D. M. Riffe[a] and A. J. Sabbah
Physics Department, Utah State University, Logan, Utah 84322-4415

(Received 26 May 1998; accepted for publication 15 June 1998)

An interferometric rapid-scanning autocorrelator employing two antiparallel rotating mirrors in a variable arm is optimized for maximum optical path difference as a function of the separation of the two rotating mirrors. A very compact design (mirror separation≈mirror diameter) is possible without a reduction in the maximum pulse width that can be measured. © *1998 American Institute of Physics.* [S0034-6748(98)05109-0]

I. INTRODUCTION

A Michelson interferometer, combined with appropriate second-order detection at the output arm, is the basis for a number of optical-pulse autocorrelator designs.[1–15] A key element in this type of autocorrelator is the design of the variable path-length arm, which depends upon a number of factors including the temporal and spectral widths of the pulses, pulse intensity, pulse repetition rate, and any requirements with regard to linearity in the time delay and compactness of the instrument. For autocorrelation measurements of unamplified pulses from femtosecond or picosecond oscillators, such as colliding-pulse mode-locked (CPM) dye lasers or Kerr-lens mode-locked (KLM) Ti:sapphire lasers, a rapid-scan arrangement, in which the path length of the variable arm is rapidly scanned, is highly desirable since it provides the basis for a real-time display of the autocorrelation signal.

Two methods are commonly used to produce a rapid scan. The first consists of mounting a retroreflector on a linear motion device such as an audio loudspeaker[4,10–12,15] or a commercial shaker[3,9,14] and driving the loudspeaker or shaker with a sinusoidal or triangular wave form. The second method consists of mounting one or several optical components on a rotating platform to obtain a path length that varies as the rotation angle of the platform is scanned.[5,6,7,13]

A nondispersive optical arrangement (suitable for femtosecond and picosecond optical pulses) that utilizes a rotating platform consists of two antiparallel mirrors mounted symmetrically about the rotation axis of the platform.[6] In this method, illustrated in Fig. 1, the light pulse from the beam splitter BS of the Michelson interferometer intercepts these two rotating mirrors (M1 and M2) and is then retroreflected from a third (stationary) mirror (M3). The beam again intercepts the two rotating mirrors on its way back to the beam splitter of the interferometer. As the platform rotation angle θ changes, the path length L of the arm is varied. The angle θ is typically scanned at a constant rate. In addition to employing nondispersive optics, this type of variable arm easily provides a path-length difference corresponding to a maximum delay of Δt of ~100 ps. Such a large path-length difference is useful even for fs lasers, since fs pulses are often stretched to ps widths before being amplified and subsequently recompressed.

However, a typical limitation of both rotating-platform and linear-drive methods is a lack of compactness. Long-throw loudspeakers are typically a minimum of 10 cm in diameter, while an earlier rotating-mirror design, which places a high priority on linearity in the scan, has the rotating mirrors separated by a large distance compared to their diameters.[6] Additionally, loudspeakers and shakers inherently produce significant amounts of vibration that can be problematic to suppress.

II. AUTOCORRELATOR DESIGN

In order to combine the desirable characteristics of nondispersive optics, large delay times, rapid scanning, minimal vibration, and compactness, we have investigated the characteristics of a rotating-mirror variable arm as a function of the separation of the two antiparallel rotating mirrors: we have independently varied both the beam height h and the mirror angle ϕ of the rotating mirrors (see Fig. 1) in order to maximize the path-length difference ΔL of the variable arm as a function of the mirror separation $2r$. Our results show that a very compact design (mirror separation $2r \approx$ mirror diameter d) is possible without any reduction in ΔL compared to that obtained at large mirror separations. The increase in nonlinearity of the scan, which necessarily results as the mirror separation $2r$ decreases, is negligible for pulse widths <1 ps and is easily correctable if quantitative analysis of longer pulse-width autocorrelation traces is required.

As shown in Fig. 1, there are four spatial points whose coordinates must be known in order to calculate the path length L of the variable arm. The points, P_1-P_4, are the four locations that the optical beam intercepts the beam splitter BS and the three mirrors M1, M2, and M3, respectively. The x and y coordinates $[P_i=(x_i,y_i)]$ of the four points can be expressed in reasonably simple form as

$$x_1 = C_1,$$

$$y_1 = h,$$

$$x_2 = h\ \tan(\phi+\theta) + r[\sin(\theta) - \cos(\theta)\tan(\phi+\theta)],$$

[a]Electronic mail: riffe@cc.usu.edu

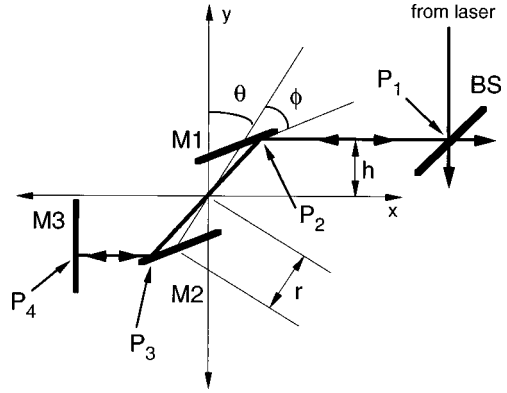

FIG. 1. Schematic diagram of rotating-mirror variable arm of the autocorrelator. The optical beam path transverses the points P1, P2, P3, and P4 and is then retroreflected back to P1. Optical components: M1 and M2 are the antiparallel rotating mirrors, M3 is a fixed mirror, and BS is the beam splitter of the Michelson interferometer. Parameters used in calculations are indicated: $r=1/2$ mirror separation, h=beam height, ϕ=mirror angle, θ=rotation angle of rotating platform.

$$y_2 = h,$$

$$x_3 = h\ \tan(\phi+\theta) + r[3-4\cos^2(\phi+\theta)] \times[\sin(\theta)-\cos(\theta)\tan(\phi+\theta)],$$

$$y_3 = h-4r\ \sin(\phi)\sin(\phi+\theta),$$

$$x_4 = C_2,$$

$$y_4 = h-4r\ \sin(\phi)\sin(\phi+\theta).$$

The origin is taken to be the axis of rotation of the mirrors M1 and M2 and the constants C_1 and C_2 depend on the location of BS and M3 but have no effect on ΔL.

The difference between our present design and the earlier design of Yasa and Amer[6] is fairly simple. In the earlier design the height h is constrained by the relationship $h = r\ \sin(2\phi)$, which results in the input beam hitting the center of M1 when $\theta=0$. For that design the maximum delay results as the separation $2r$ becomes much larger than d, with a maximum round-trip path-length difference of $\Delta L \approx \sqrt{2}d$. In contrast, we have independently varied both h and ϕ to determine the maximum ΔL as a function of the separation $2r$ between the mirrors.

III. NUMERICAL RESULTS

Our results, numerically derived, are shown in Fig. 2. The results shown are for $d=2.54$ cm, a standard mirror diameter. For an autocorrelator employing rotating mirrors with a different diameter, all linear dimensions and delay times shown here can be scaled by size of the rotating mirrors relative to our 2.54 cm diam. Parts (a) and (b) of Fig. 2 plot the mirror angle $\phi_{\max}$ and beam height $h_{\max}$ that maximize the delay time $\Delta t=\Delta L/c$ (c=speed of light) as a function r. Surprisingly, the maximum delay time of 122 ps occurs for $r\approx d$. However, even for $2r$ as small as d, Δt is still larger than the maximum delay of $\sqrt{2}d/c=120$ ps of the earlier design.[6] For large values of r our delay approaches the earlier design result of 120 ps.

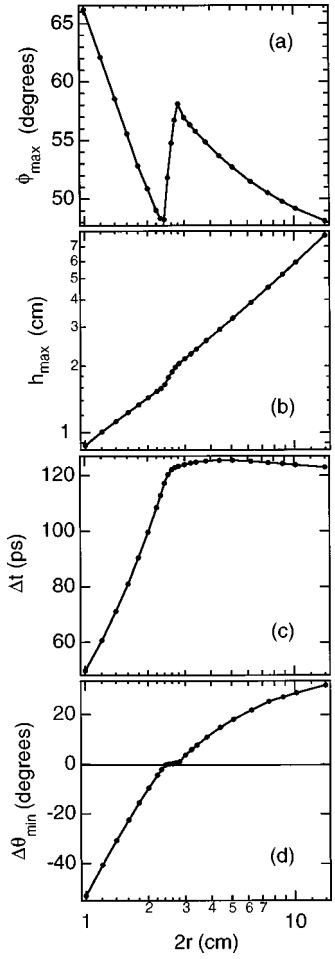

FIG. 2. Results of calculations optimizing the mirror angle ϕ and beam height h for maximum delay time Δt as a function of the mirror separation $2r$. (a) Optimum mirror angle $\phi_{\max}$. (b) Optimum beam height $h_{\max}$. (c) Resultant delay time Δt for corresponding $\phi_{\max}$ and $h_{\max}$. (d) Difference in minimum rotation angle conditions $\Delta\theta_{\min}=\theta_{\min,2}-\theta_{\min,1}$ (see the text for details).

As is evident in Fig. 2, both $\phi_{\max}$ and $h_{\max}$ show interesting structure near $2r=2.6$ cm. This behavior is related to the specific condition that determines the minimum rotation angle $\theta_{\min}$. For small mirror separations ($2r<2.54$ cm) $\theta_{\min}$ occurs when the beam hits the lower edge of M1, as illustrated in Fig. 3(a) where this condition on $\theta_{\min}$ is denoted $\theta_{\min,1}$. For larger mirror separations $\theta_{\min}$ is determined by the condition that P_3 is at the upper edge of M2, as shown in Fig. 3(b) where $\theta_{\min}$ is denoted $\theta_{\min,2}$. The structure in $\phi_{\max}$ and $h_{\max}$ occurs as the minimum-angle condition crosses over from $\theta_{\min,1}$ to $\theta_{\min,2}$ as r is increased. This behavior is emphasized in part (d) of Fig. 2, which plots the difference in angle $\Delta\theta_{\min}=\theta_{\min,2}-\theta_{\min,1}$, where these two conditions occur as a function of $2r$. As shown in Fig. 2(d), in the crossover region, which occurs for $2r$ between 2.4 and 2.8 cm, $\theta_{\min,1}$ and $\theta_{\min,2}$ are nearly identical.

The one drawback of the current design, compared to the earlier design in which d is much smaller than r, is an increased nonlinearity in Δt versus θ. The nonlinearity NL over the whole scan can be estimated from $NL\approx d/8r$,[6] which for $d=2r$ is $\sim$25%. For pulse widths of 10 ps this results in a $NL\approx 4\%$. For pulses in the fs regime the nonlin-

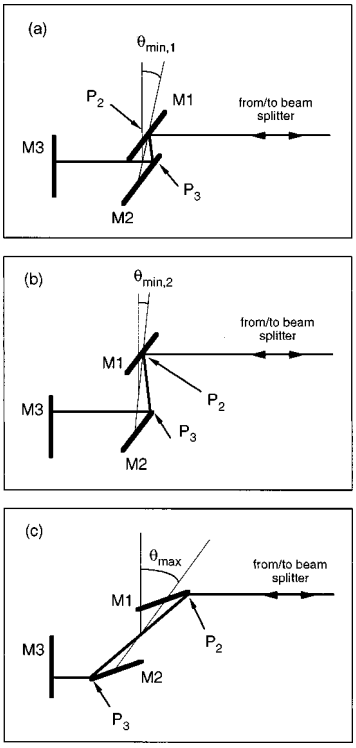

FIG. 3. Minimum and maximum rotation angle conditions. (a) Conditions for minimum rotation angle ($\theta_{\min,1}$) for small mirror separations. (b) Conditions for minimum rotation angle ($\theta_{\min,2}$) for large mirror separations. (c) Condition for $h_{\max}$ at the maximum mirror rotation angle $\theta_{\max}$ (see the text for details).

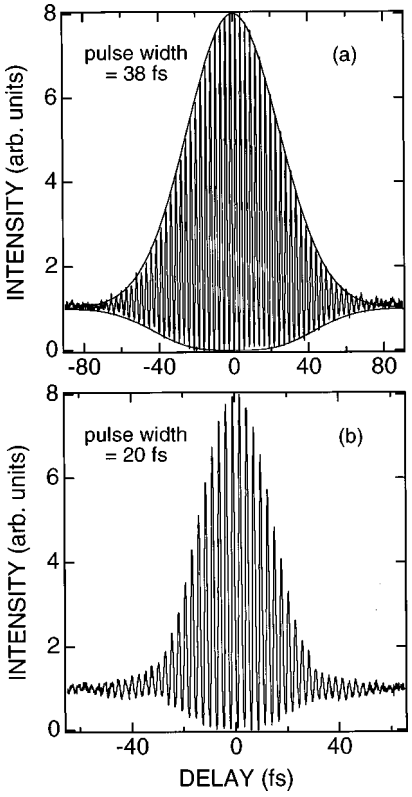

FIG. 4. Interferometric autocorrelation traces from a Ti:sapphire oscillator. (a) Autocorrelator trace from laser pulses consistent with a Gaussian pulse shape and FWHM=38 fs. Theoretical envelope curves for a Gaussian pulse are also shown. (b) Autocorrelator trace from laser pulses with a FWHM of ~20 fs.

earity is entirely negligible: for example, for a 100 fs pulse $NL \approx 0.04\%$. If a highly accurate autocorrelation trace in the super-ps regime is required, the nonlinearity can be accurately assessed using an interferogram from a cw laser with linear detection at the output of the Michelson interferometer.

Optical-component alignment of the variable arm is straightforward. After determining and setting the desired separation $2r$ of the rotating mirrors, the optimum mirror angle $\phi_{\max}$ is adjusted to the value shown in Fig. 2(a). The next adjustment is the input beam height $h_{\max}$. While $h_{\max}$ can be determined from the graph in Fig. 2(b), it can also be located by adjusting the beam height h until, at the maximum value of the rotation angle θ (which occurs when P_3 is at the lower edge of M2) the point P_2 is at the upper edge of M1, as shown in Fig. 3(c). In fact, using this condition on P_2 results in a relatively simple equation for $h_{\max}$ as a function of r, d, and ϕ:

$$h_{\max}=\frac{2r\ \sin(\phi)}{\sqrt{(d/2)^2+dr\ \cos(\phi)+r^2}}\left[\frac{d}{2}+r\ \cos(\phi)\right].$$

Note that this equation gives the value of h that maximizes Δt even if ϕ has not been optimized to $\phi_{\max}$.

IV. EXPERIMENTAL RESULTS

We have utilized our rotating-mirror design in an interferometric autocorrelator, which we use to measure pulses from an in-house constructed Ti:sapphire oscillator.[16] In our particular implementation of the autocorrelator design we have slightly emphasized compactness over maximum time delay and have chosen $2r=2.0$ cm, which results in a maximum $\Delta t=100$ ps for $\phi_{\max}=51°$ and $h_{\max}=1.4$ cm. For detection at the output of the interferometer we use an AlGaAs (light-emitting) diode, which provides a second-order output since absorption of two photons is necessary to excite a valence electron into the conduction band.[17] Use of such a diode also enhances the compactness and cost effectiveness of the autocorrelator compared to using a nonlinear optical crystal, optical filter, and photomultiplier arrangement for second-order detection. The diode output is amplified and sent to a digitizing oscilloscope that records the autocorrelation trace. In our autocorrelator the mirror rotation frequency is ~1 Hz, requiring a detection bandwidth of ~1 MHz for interferometric autocorrelation.

Two typical autocorrelation traces of Ti:sapphire oscillator pulses that have been measured with our autocorrelator are shown in Fig. 4. The top trace is indicative of Gaussian-shaped pulses with a full width at half maximum (FWHM) of 38 fs. The second trace, which is from the same Ti:sapphire oscillator after a small translation of one of the internal dispersion-controlling prisms, is consistent with a FWHM of ~20 fs but no longer exhibits a Gaussian pulse shape. Note that each trace is from a single pass of the variable arm. The clean interference fringes of both traces demonstrate the inherent mechanical stability of the design.

V. DISCUSSION

In summary, we have described a compact rotating-mirror autocorrelator design, useful for both fs and ps pulses, that significantly reduces the overall size requirements of the autocorrelator compared to other rotating platform and linear-drive designs, but at the same time retains a large scan range suitable for pulses up to several tens of picoseconds long.

[1] J. A. Armstrong, Appl. Phys. Lett. **10**, 16 (1967).
[2] H. P. Weber, J. Appl. Phys. **38**, 2231 (1967).
[3] R. L. Fork and F. A. Beisser, Appl. Opt. **17**, 3534 (1978).
[4] K. L. Sala, G. A. Kenny-Wallace, and G. E. Hall, IEEE J. Quantum Electron. **QE-16**, 990 (1980).
[5] Y. Ishida, T. Yajima, and Y. Tanaka, Jpn. J. Appl. Phys., Part 2 **19**, L289 (1980).
[6] Z. A. Yasa and N. M. Amer, Opt. Commun. **36**, 406 (1981).
[7] H. Harde and H. Burggraf, Opt. Commun. **38**, 211 (1981).
[8] T. Kurobori, Y. Cho, and Y. Matsuo, Opt. Commun. **40**, 156 (1981).
[9] A. Kalpaxis, A. G. Doukas, Y. Budansky, D. L. Rosen, A. Katz, and R. R. Alfano, Rev. Sci. Instrum. **53**, 960 (1982).
[10] A. Watanabe, M. Hirose, H. Terane, S. Tanaka, H. Kobayashi, and M. Hara, Rev. Sci. Instrum. **55**, 262 (1984).
[11] P. Myslinski, Rev. Sci. Instrum. **58**, 711 (1987).
[12] A. Watanabe and H. Saito, Rev. Sci. Instrum. **58**, 1852 (1987).
[13] G. Xinan, M. Lambsdorff, J. Kuhl, and W. Biachang, Rev. Sci. Instrum. **59**, 2088 (1988).
[14] A. Watanabe, H. Saito, Y. Ishida, and T. Yajima, Opt. Commun. **69**, 405 (1989).
[15] J. A. I. Oksanen, V. M. Helenius, and J. E. I. Korppi-Tommola, Rev. Sci. Instrum. **64**, 2706 (1993).
[16] M. T. Asaki, C.-P. Huang, D. Garvey, J. Zhou, H. C. Kapteyn, and M. M. Murnane, Opt. Lett. **18**, 977 (1993).
[17] D. T. Reid, M. Padgett, C. McGowan, W. E. Sleat, and W. Sibbett, Opt. Lett. **22**, 233 (1997).